

Study on fatigue life and mechanical properties of BRBs with viscoelastic filler

Zhao-Dong Xu^{*1}, Jun Dai^{1a} and Qian-Wei Jiang^{2b}

¹ Key Laboratory of C&PC Structures of the Ministry of Education, Southeast University, Nanjing 210096, China

² Longyan Electric Power Survey and Design Institute Co. LTD, Longyan 350003, China

(Received May 26, 2017, Revised September 21, 2017, Accepted October 4, 2017)

Abstract. In this paper, two kinds of buckling restrained braces (BRBs) are designed to improve the mechanical properties and fatigue life, the reserved gap and viscoelastic filler with high energy dissipation capacity are employed as the sliding element, respectively. The fatigue life of BRBs considering the effect of sliding element is predicted based on Manson-Coffin model. The property tests under different displacement amplitudes are carried out to evaluate the mechanical properties and fatigue life of BRBs. At last, the finite element analysis is performed to study the effects of the gap and viscoelastic filler on mechanical properties BRBs. Experimental and simulation results indicate that BRB employed with viscoelastic filler has a higher fatigue life and more stable mechanical property compared to BRB employed with gap, and the smaller reserved gap can more effectively improve the energy dissipation capacity of BRB.

Keywords: buckling restrained brace; fatigue life; mechanical property; viscoelastic material

1. Introduction

In recent decades, structural vibration control has been one of the most considerable topics in the field of civil engineering, and the passive control is a reliable and mature technology (Soong and Dargush 1997). Buckling restrained brace (BRB) as a representative displacement-type passive damper has been widely used in practical engineering due to its good energy dissipation capacity (Soong and Spencer 2002).

BRB consists of three components: inner core element, outer restrained element and sliding element. The inner core element is the energy consumption part of BRB, and the section from determines the energy dissipation capacity. The common section of core element includes rectangular section, crisscross section, H-section and composite section (Xie 2005). The reasonable design of the outer restrained element is a prerequisite for the normal operation of the core element. Zhao *et al.* (2011) designed a new type of angel steel BRB, the restrained element was a steel tube welded longitudinally by two angel steels. Takeuchi *et al.* (2012) investigated the effects of mortar thickness and the restraint tube shape on the local buckling failure of BRBs. Abdollahzadeh and Banihashemi (2013) evaluated the effect of BRB configurations on the response modification factor. Kim *et al.* (2014) designed a hybrid BRB with viscoelastic dampers to control the wind-induced vibration of tall buildings, and the time-history analysis verified the

effectiveness of the hybrid BRB system. Ghowsi and Sahoo (2015) investigated the effects of the brace configurations and connections on the seismic response of a medium-rise frame under the near-fault ground motions.

The sliding element is employed to improve mechanical performance of BRB, and the reserved gap and unbonding materials (UMs) are the common forms. Ding *et al.* (2009) designed a panel BRB comprised of un-bonded steel brace and reinforced concrete panel, the test results showed that the UMs had great effects on the hysteretic behavior of the BRB. Chou and Chen (2010) studied the feasibility of a small gap substituting UM, the experimental result showed the gap slightly affects the cyclic behavior of the proposed BRB. Park *et al.* (2012) used the continuous steel rod to fill the gap between the core and the tube and obtained the better mechanical performance of BRB. Wang *et al.* (2012) conducted a low-cycle fatigue experiment of BRBs, the test result showed that the toe-finished method effectively improves the BRB's low-cycle fatigue performance. Tsai *et al.* (2014) tested four BRB specimens with different UMs and found that the UMs can reduce the difference between the cyclic peak compression and tension. Talebi *et al.* (2015) investigated the effects of the size and type of fill materials on the fire resistance capacity of BRB. Chen *et al.* (2016) found that the BRB with UM has a good energy dissipation capacity and lower compression strength adjustment factor. Bregoli *et al.* (2016) and Metelli *et al.* (2016) studied the thrust generated by core bucking of BRB and found the gap dimension plays as significant role on the lateral thrust. Most of studies focus on the effect of the sliding element on the energy dissipation capacity of BRB, the mechanical stability and fatigue life are also important for BRBs but related studies are not sufficient.

In order to improve fatigue life and mechanical stability

*Corresponding author, Professor,
E-mail: zhdxu@163.com

^a Ph.D. Candidate, E-mail: daijun4242@163.com

^b Research Assistant, E-mail: jiangqian_wei@163.com

of BRBs, viscoelastic material with high energy dissipation capacity (Xu *et al.* 2011 and 2016, Gong and Zhou 2016) is used as the UM of BRB. In this paper, BRBs with 0.5 mm gap and with 2 mm viscoelastic filler are manufactured, and then the fatigue life prediction models of the two BRBs are proposed. To evaluate the fatigue performance and mechanical properties of the two BRBs, property tests under different loading amplitudes are carried out. Considering the effects of the reserved gap and viscoelastic filler, the finite element analysis of the new type of BRB is also performed.

2. BRB Configuration

Two kinds of BRBs with identical dimension are designed, as shown in Fig. 1. One specimen is the all-steel assembled BRB reserving 0.5 mm gap between the core element and restrained element, which is named BRB1. The other one is the all-steel assembled BRB with 2 mm viscoelastic filler, which is named BRB2.

2.1 Inner core element

In this study, the widely used and inexpensive Q235 steel is used to make the inner core element of BRB, and the material test is conducted according to GB/T228-2002. The tensile strength/yield strength ratio of Q235 steel reaches 1.37, which is able to provide adequate security. The elongation of the core steel reaches 27.6%, which is much longer than the usual 3% axial strain of BRB. The core section and core length are determined according to the requirements of AISC (2010) and the limits of test

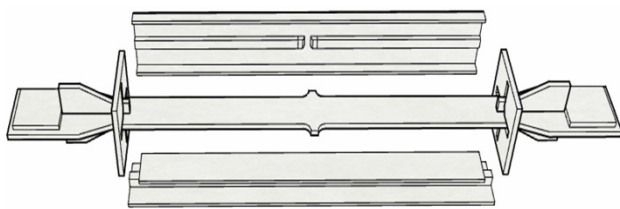


Fig. 1 Composition of BRB

- *a: Energy dissipation section
- *b: Outer restrained element
- *c: Transition section
- *d: Connection section
- *e: Viscoelastic filler
- *f: Welding steel
- *g: Stiffener

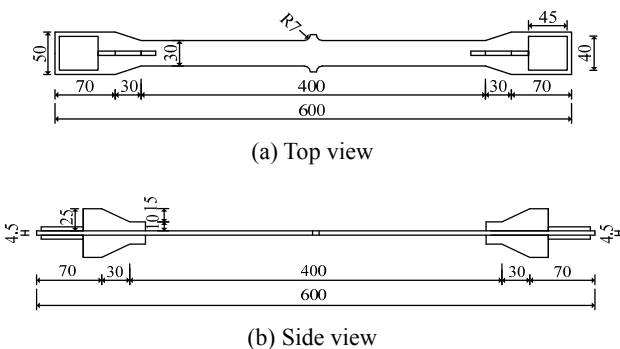


Fig. 2 Geometry dimensions of inner core element

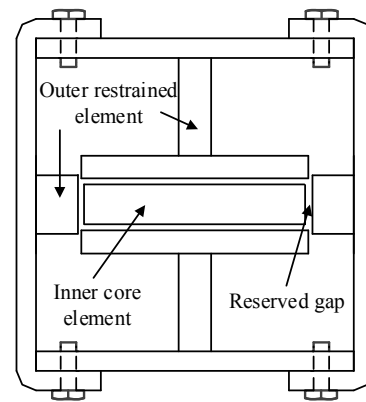
condition, and Fig. 2 shows the geometric dimensions of the inner core element. To avoid the connection section being destroyed before the energy dissipation section, the stiffener and welding steel are disposed out of the plane of the transition section.

2.2 Outer restrained element

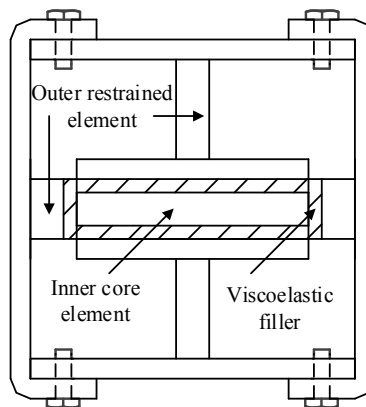
Outer restrained element must have sufficient bending stiffness to limit the wave-like deformation of the core element. The two BRBs both adopt a combination of shaped steel, which is connected by bolts, as shown in Fig. 3. This full assembly form can realize the replacement of the core element when BRB fails to work. The case stiffness of BRB should be large enough to prove the overall stability of BRB, and the constraint ratio proposed by Watanabe *et al.* (1988) is often used as an evaluation index. The constraint ratios of the two BRBs both reach 35, which is much larger than the suggested critical value of 1.3.

2.3 Viscoelastic filler

The UM employed in BRB2 is a new type of viscoelastic material based on nitrile rubber, which is developed by our research group (Xu *et al.* 2016). The viscoelastic material has a high energy dissipation capacity over the frequency range 0.1 Hz to 10 Hz, and can effectively mitigate various vibrations and deformations.



(a) BRB1



(b) BRB2

Fig. 3 Cross sections of BRBs

Table 1 Physical parameters of viscoelastic filler

Hardness (HA)	Tensile strength (MPa)	Elongation (%)	Elasticity modulus (MPa)	Poisson's ratio
76	12.2	440	5.00	0.495



Fig. 4 Viscoelastic filler

Some physical parameters of the viscoelastic material are listed in Table 1. The high elongation of 440%, the sufficient hardness and tensile strength all indicate that the filler is suitable for the sliding element of BRB. The viscoelastic filler is adhered to outer restrained elements with epoxy, as shown in Fig. 4.

3. Prediction model on fatigue life

The stress-life approach and the strain-life approach are common approaches to evaluate the fatigue life of steel, and the strain-life approach is used to predict the fatigue life of two BRBs in this paper.

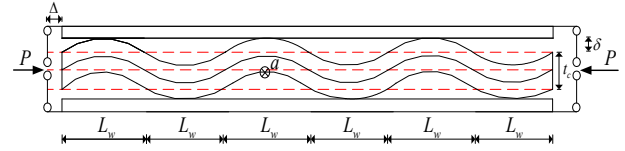
The energy consumption section of the core element will generate yielding plastic deformation when BRB is under the repeated tensile and compressive loading, which is a typical low-cycle fatigue problem. The Manson-Coffin model (Coffin 1954, Manson 1965) is used to predict the fatigue life of BRBs.

$$\frac{\Delta\varepsilon}{2} = \frac{\sigma'_f}{E} (N)^{c_1} + \varepsilon'_f (N)^{c_2} \quad (1)$$

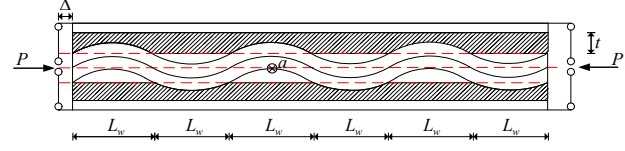
where c_1 is fatigue strength exponent, c_2 is exponent of the fatigue plastic strain, N is the number of stress cycles to fracture, σ'_f is the coefficient of the fatigue strength under tension and compression, ε'_f is the coefficient of fatigue plasticity, $\Delta\varepsilon$ is the amplitude of strain. The expression of strain-fatigue life curve of Q235 steel is

$$\Delta\varepsilon = 0.0066(N)^{-0.071} + 0.549(N)^{-0.4907} \quad (2)$$

Actually, the BRB is always working under different amplitudes. The fatigue damage can be considered as linear combination of fatigue damage at different amplitudes according to the classical Miner theory, and the Miner's rule (Miner 1945) is given by



(a) BRB1



(b) BRB2

Fig. 5 Deformation of inner core element of BRBs

$$D = \sum_{i=1}^m \frac{n_i}{N_i} \quad (3)$$

where D is the cumulative fatigue damage, m is the number of load amplitude, N_i is the fatigue life for the i th load amplitude. If the average fatigue damage of each cycle at the i th load amplitude is $1/N_i$, then the fatigue damage of n_i cycles is n_i/N_i . The specimen will fail in working when the cumulative damage D reaches a critical value of 1.

3.1 All-steel assembled buckling restrained brace

The strain of the inner core element is not uniformly distributed along the length due to the effect of the multi-wave buckling deformation. The maximum strain point determines fatigue life of BRBs, which is a point in Fig. 5(a). As the multi-wave buckling deformation of the inner core element is symmetrical, the inflection point of bending is located at the neutral disposition of the inner core element. The mathematical model of multi-wave buckling can be simplified to half-wave buckling connected by hinges, as shown in Figs. 6(a) and (b).

According to the tangent modulus theory of compression members in plastic state, the length of half-wave L_w is

$$L_w = \pi t_c \sqrt{\frac{E_t b t_c}{12P}} \quad (4)$$

where $E_t = 0.02E$ is the tangent modulus of Q235 steel and E is the elastic modulus of Q235 steel, b and t_c are the width and thickness of section of the core element. The curve of the half-wave is assumed as

$$y = \delta \sin\left(\frac{\pi x}{L_w}\right) \quad (5)$$

where δ is the gap between the core element and the restrained element. The maximum compressive strain of point a includes the axial compression deformation ε and bending deformation ε_w

$$\varepsilon_{\max} = \varepsilon + \varepsilon_w \quad (6)$$

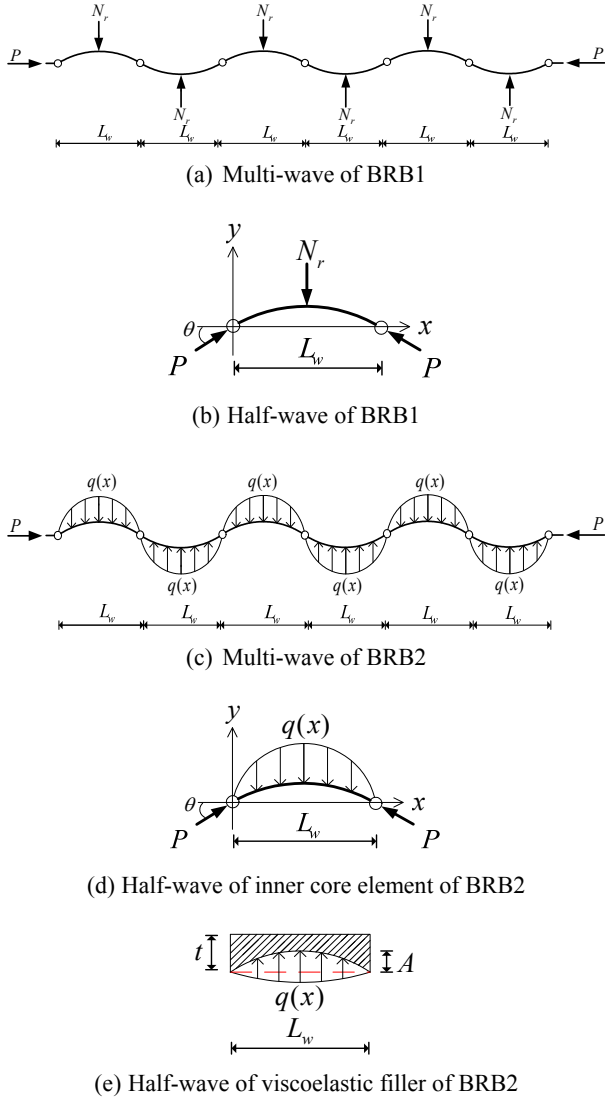


Fig. 6 Mathematical model of inner core element of BRBs

$$\varepsilon_w = \phi \frac{t_c}{2} = -y'' \frac{t_c}{2} \quad (7)$$

where ϕ is the curvature of point a obtained from the second derivation of Eq. (5), and then Eq. (7) can be rewritten as

$$\varepsilon_w = \frac{\delta \pi^2 t_c}{2L_w^2} \quad (8)$$

Thus, the maximum strain amplitude of BRB1 in low-cycle fatigue loading can be written as

$$\Delta \varepsilon = 2\varepsilon + \frac{\delta \pi^2 t_c}{2L_w^2} \quad (9)$$

The cumulative damage D of BRB1 competing a loading stage can be calculated according to Eqs. (2), (3) and (9). The predicted loading stage is defined to characterize the fatigue life of BRB, which is actually the

number of the loading stage making the cumulative damage reach a critical value of 1, i.e., the reciprocal of D . It is noted that the defined loading stage here is consistent with that in Section 4.1. The cumulative damage is 0.193 when BRB1 completes a loading stage, and the number of predicted loading stage is 5.18 according to Miner's rule, which is shown in Table 3.

3.2 Buckling restrained brace with viscoelastic filler

The deformation of the inner core element of BRB2 is not the same as that of BRB1, which is shown in Fig. 5(b). The mathematical model of multi-wave buckling can be simplified as shown in Figs. 6(c), (d) and (e). The length of half-wave is the same as that of BRB1, and the curve of the buckling half-wave is assumed as

$$y = A \sin\left(\frac{\pi x}{L_w}\right) \quad (10)$$

where A is the amplitude of the half-wave curve. The balance of force in y -direction can be written as

$$2P \sin \theta = \int_0^{L_w} q(x) dx \quad (11)$$

According to the definition of the voluminal modulus of viscoelastic material

$$K = \frac{p}{\Delta} \quad (12)$$

where p is average compressive stress, Δ is volume compressive strain, which can be calculated from the following equations

$$p = \frac{\int_0^{L_w} q(x) dx}{bL_w} \quad (13)$$

$$\Delta = \frac{\Delta V}{V} = \frac{b \int_0^{L_w} y dx}{btL_w} \quad (14)$$

According to Eqs. (10)-(14), the amplitude of half-wave buckling is given by

$$A = \frac{\pi P t \sin \theta}{L_w b K} \quad (15)$$

The rotation θ locating at $x = 0$ can be obtained from first derivation of Eq. (10), and then θ is taken into Eq. (15)

$$\theta = y' \Big|_{x=0} = \frac{A \pi}{L_w} \quad (16)$$

$$\left(\frac{K}{t}\right) \frac{L_w b}{P \pi} A = \sin \frac{\pi A}{L_w} \quad (17)$$

It can be seen from Eq. (17) that the amplitude A is dependent on voluminal modulus and thickness of

viscoelastic filler. In fact, the voluminal modulus can be expressed as

$$K = \frac{E_v}{3(1-2\nu)} \quad (18)$$

where ν is the Poisson's ratio of the viscoelastic material.

The strain amplitude of BRB2 can be obtained from Eqs. (6), (7) and (10)

$$\Delta\varepsilon = 2\varepsilon + \frac{A\pi^2 t_c}{2L_w^2} \quad (19)$$

The theoretical fatigue life of BRB2 is listed in Table 3. The cumulative damage is 0.173 when BRB2 completes one loading stage, and the number of predicted loading stage is 5.78 according to Miner's rule.

4. Experimental verification

4.1 Experimental setup

In order to evaluate the mechanical properties and fatigue life of the two types of BRBs, the fatigue tests were conducted. The tests were carried out on a servo-hydraulic fatigue test machine with ± 800 kN dynamic loading force and ± 75 mm piston stroke, as shown in Fig. 7. The test data was collected by the force sensor and displacement sensor on the actuator.

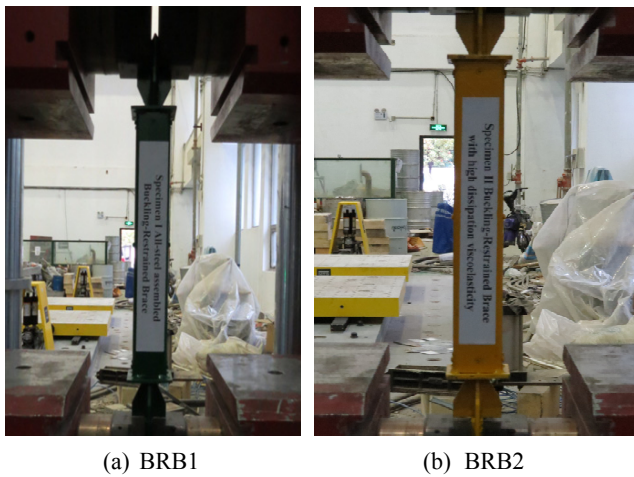


Fig. 7 Experimental setups

Table 2 Loading stages of the experiment

Loading stage	Axial strain (%)	Displacement (mm)	Ductility	Cycles
$i = 1-5$	0.50	2	4.40	10
	0.75	3	6.60	10
	1.00	4	8.80	10
	1.50	6	13.2	10

Table 3 Experimental and theoretical prediction loading stages

Specimen	Theoretical result	Experimental result	Percentage error
BRB1	5.18	4.36	15.8
BRB2	5.78	4.76	17.6
Smooth	31.3	—	—

The test program consists of the two phases. First, the BRB was pre-tensioned with 1 mm axial displacement and then was reversely loaded back to the origin position, this purpose of the operation is to reduce the possible slippage of chucks. Second, the two BRBs are loaded with 10 cycles of sine wave under different displacement amplitudes and the total 40 cycles are defined as a loading stage. 5 identical loading stages are sequentially conducted until the BRB is destroyed. Table 2 shows the detailed test program.

4.2 Fatigue life

The two BRBs were loaded according to the test program in Table 2, and stages of failure were recorded. The comparison between experimental and theoretical prediction loading stages of BRBs is listed in Table 3. It is found that experimental results satisfy with theoretical prediction well, and the error below 20% can be accepted. The residual stress and initial bending of BRB lead to the less fatigue life compared with the theoretical calculation. If only the axial deformation of the core element is considered, the number of predicted loading stage of BRB1 is 31.3, which indicates the multi-wave buckling deformation significantly affects the fatigue life of BRBs and cannot be ignored. Compared to the experimental result of BRB1, the viscoelastic filler in BRB2 can improve the fatigue life of BRB by 9.2%. The reason is that the viscoelastic filler in BRB2 effectively mitigates the multi-wave buckling deformation of the core element.

4.3 Mechanical properties

4.3.1 Hysteresis curve

Hysteresis curve can comprehensively reflect the hysteretic energy capacity, and the fuller curve means the better hysteretic energy capacity of BRBs. Hysteresis curves of BRB1 are plotted in Fig. 8. In the first stage, the hysteretic curves are extremely full and behave symmetrically, and the provided stiffness is sufficient in tension and compression. However, the hysteretic curves are gradually asymmetrical and the compressive capacity jumps markedly in the next loading stages. The reason for the phenomenon is that the 0.5 mm gap may results in the tiny local buckling of the core element and then reduces the compression bearing capacity, but the local buckling will be limited by the restrained element with the increase of the amplitude. Hysteresis curves of BRB2 are plotted in Fig. 9. The hysteretic curves are relatively full and stable in each loading stage, which exhibits a better mechanical stability. This advantage is derived from that the lateral protection provided by the viscoelastic filler effectively weakens the local buckling of the core element.

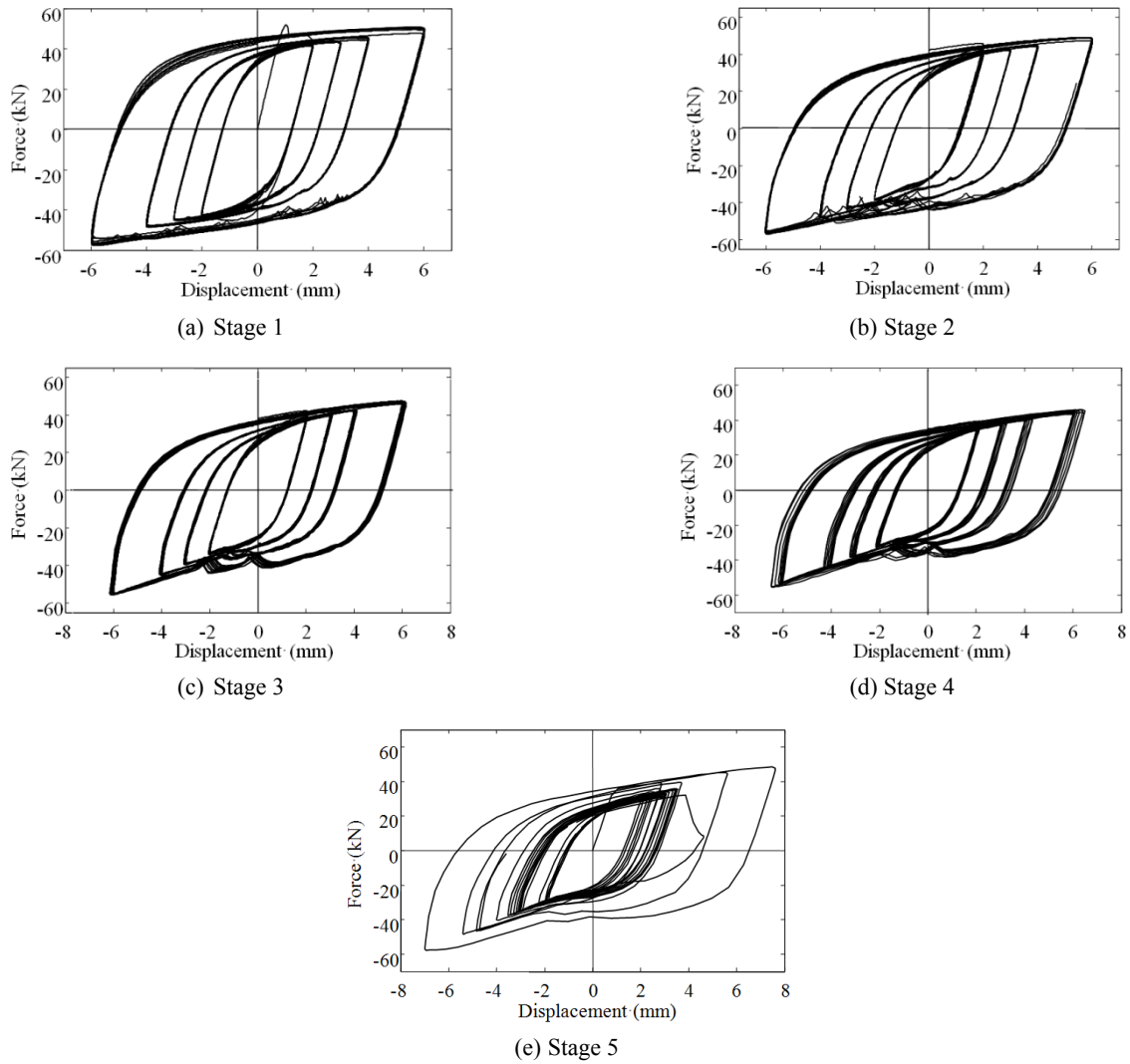


Fig. 8 Hysteresis curves of BRB1

It is noted that BRB2 has a remarkable pinching effect and a lower maximum compressive axial force for a given axial strain. This is because the thickness or the placement of the viscoelastic filler is not well designed. But it cannot be concluded that the hysteretic energy capacity of BRB1 is superior to that of BRB2, the thicknesses of the gap and the viscoelastic filler are not the same, and the reasonable comparison will be conducted in Section 5.3.

4.3.2 Stability of energy dissipation

In order to further compare the stability of energy dissipation of the two BRBs, the cumulative plastic deformation (CPD) and stability coefficient of energy dissipation η are proposed as

$$\text{CPD} = \sum_{i=1}^n [2(|\Delta_{\max}| + |\Delta_{\min}|) / \Delta_y - 4] \quad (20)$$

$$\eta = \frac{E_d}{E_{d,1}} \quad (21)$$

where Δ_{\max} is the maximum displacement in the compress-

sion state, Δ_{\min} is the maximum displacement in the tension state, Δ_y is the yield displacement, n is the number of the cycle, $n = 10$ in this paper. CPD is calculated and added in sequence according to the loading history in Table 3, as total of 20 data. E_d is the area of hysteretic curve at the same load amplitude, $E_{d,1}$ is the area of hysteretic curve at the first loading stage, and the typical curve (the fifth curve of the ten curves) is selected to calculate η . Fig. 10 plots the variations of η with the CPD at different amplitudes. As can be seen, η of two BRBs both decrease with the increase of CPD (or the loading stage), which is mainly due to the degradation of stiffness of the core element. In detail, η of BRB2 changes little with the increase of CPD after the first loading stage, but η of BRB1 continues to decrease with the increase of CPD. As a result, BRB1 is destroyed earlier than BRB2 in the test. Considering the working condition of BRBs (removing the points at the first loading stage and failure stage), η of BRB1 respectively decrease 10.1%, 12.7%, 12.6% and 11.2% at the amplitudes of 2 mm, 3 mm, 4 mm and 6 mm, but those of BRB2 decrease only 9.2%, 3.8%, 8.2% and 6.8%. The advantages of BRB2 on energy dissipation stability is due to that, the viscoelastic filler eases the slight fluctuations of the core element in the

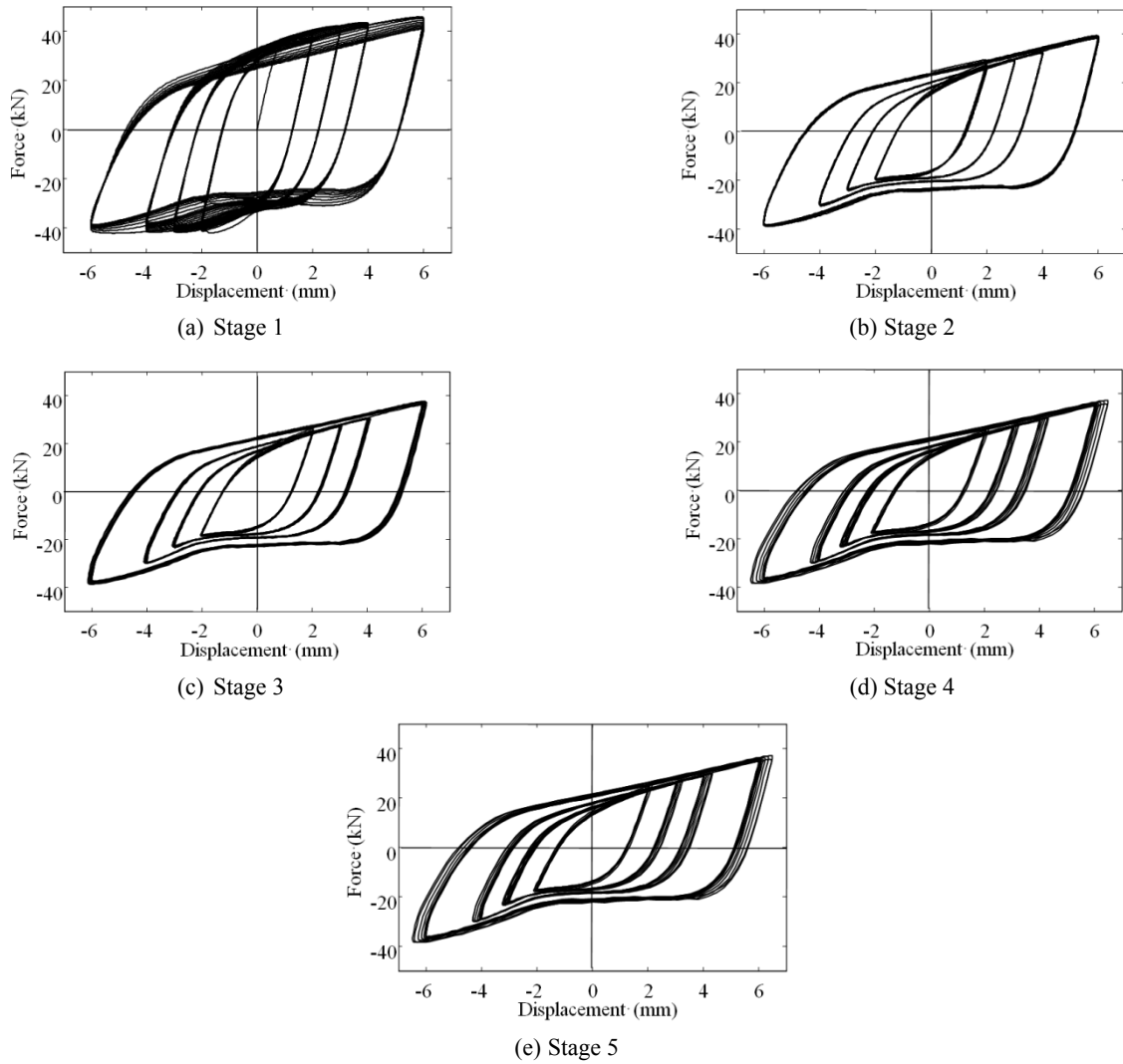


Fig. 9 Hysteresis curves of BRB2

compression state and then the limited local deformation postpones the degradation of stiffness. Meanwhile, the extrusion provided by the core element can lead to the additional energy dissipation of viscoelastic filler.

4.3.3 Symmetry in tension and compression

Unbalanced coefficient is always used to describe the asymmetrical behavior of BRBs in tension and compression, which is expressed as

$$\beta = \frac{P_{c,\max}}{P_{t,\max}} \quad (22)$$

where $P_{c,\max}$ is the maximum compressive loading capacity, $P_{t,\max}$ is maximum tensile loading capacity, and the typical curve (the fifth curve of the ten curves) is selected to calculate β . Fig. 11 plots the variations of β with the CPD at different amplitudes. As can be seen, the change of β with the CPD is not obvious, because β is more related to the frictional force between the core element and the restrained element, and the constraint effect of the restrained element on the core element. The effect of CPD on the unbalance

coefficient is small, thus this trend is not always increasing. The maximum β of BRB1 increases with the increase of the load amplitude, 1.02, 1.123, 1.203 and 1.216 at the amplitudes of 2 mm, 3 mm, 4 mm and 6 mm. This is because the higher order multi-wave buckling increases the contact area between the core element and the restrained element, and then makes BRB1 behave asymmetrical in tension and compression at the large load amplitude. The maximum β of BRB2 are 0.99, 0.952, 1.075 and 1.044 at the amplitudes of 2 mm, 3 mm, 4 mm and 6 mm, and the maximum reduction ratio is 16.5% compared to BRB1. This is because viscoelastic filler provides the expansion space for the core element, and reduces the friction between the core element and the restrained element.

5. Effects of reserved gap and viscoelastic filler

In order to further analyze the effects of the reserved gap and the viscoelastic filler on the mechanical properties of BRBs, the finite element analysis of BRBs was performed.

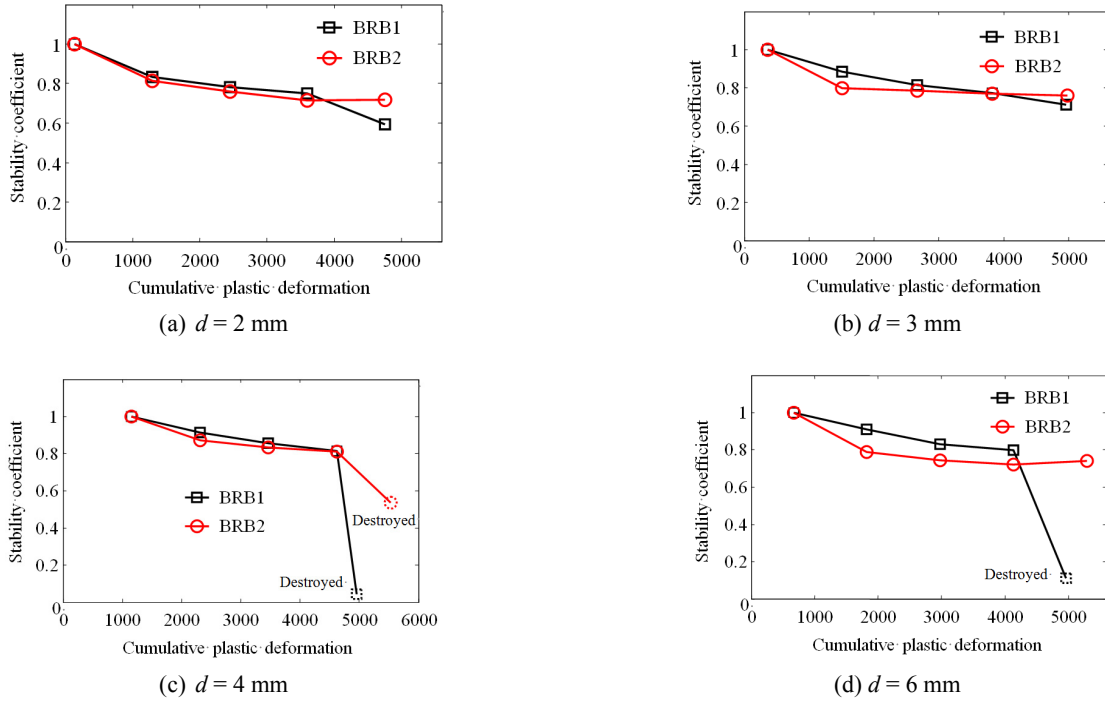


Fig. 10 Variations of stability coefficient with cumulative plastic deformation

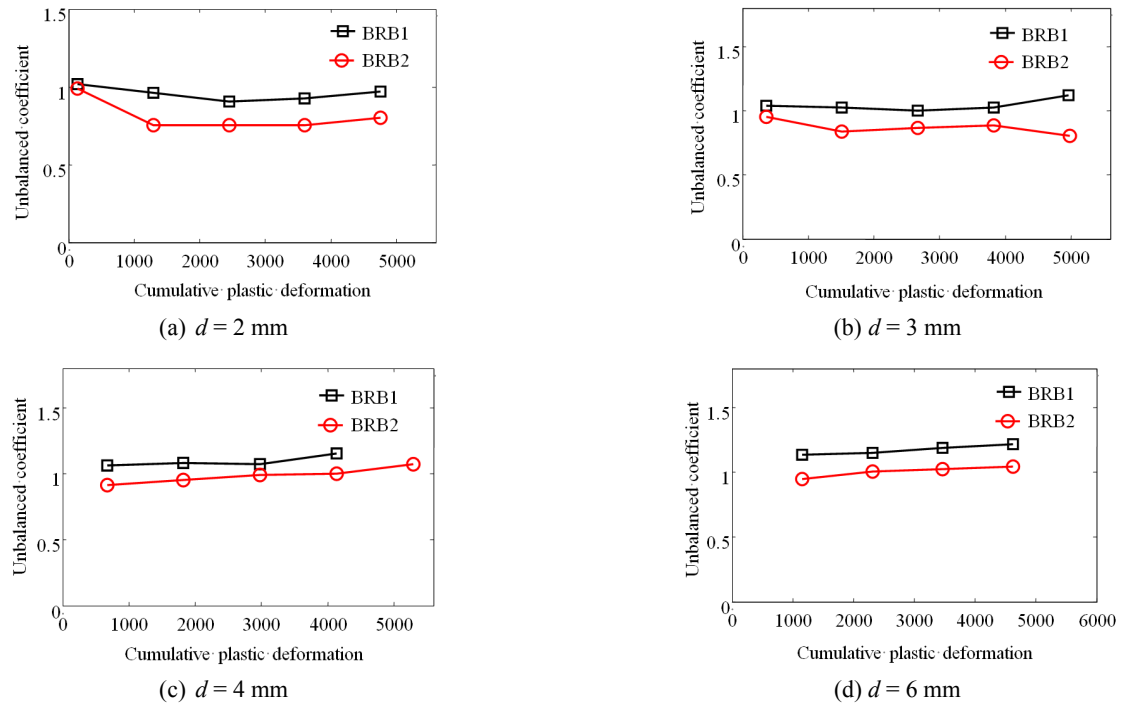


Fig. 11 Variations of unbalanced coefficient with cumulative plastic deformation

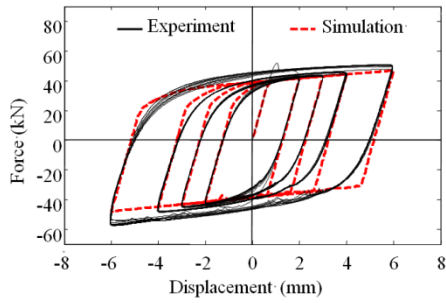
5.1 Establishment of finite element model

The finite element model of BRB1 was established using ANSYS software. The eight-node solid element SOLID45 is used to simulate the steel, the element size is defined as 5mm to prove the convergence and accuracy of calculation. The interface elements CONTA174 and TARGE170 are used to simulate the surface contacts

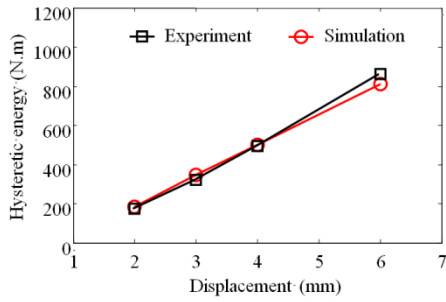
between the core element and the restrained element. The bilinear kinematic hardening model is used to model the material property of steel. The initial defect of the core element is simulated by applying a 1/1000 initial bending.

Compared to the test program, this simulation is simplified as only a loading circle at four amplitudes of 2 mm, 3 mm, 4 mm and 6 mm, respectively. Fig. 12 shows the comparison between simulation and experimental

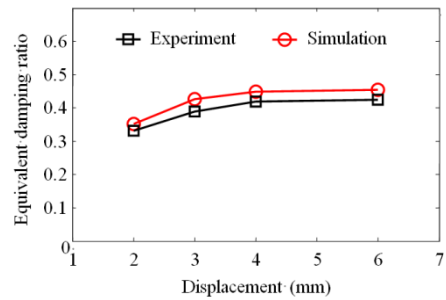
results of mechanical properties of BRB1 with 0.5 mm gap. It can be seen that hysteresis curves are full and agree well with each other, which indicates that the established finite element model can effectively simulate the mechanical properties of BRB1. The hysteretic energies and the equivalent damping ratios are close at different load amplitudes and their maximum errors are 5.9% and 8.8%, which means that the simulation result slightly enlarges the energy dissipation capacity of BRB1.



(a) Hysteresis curve

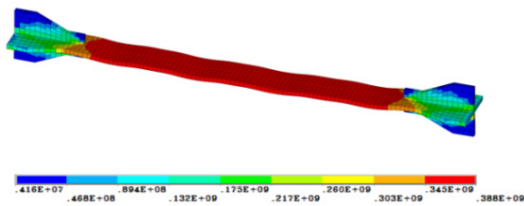


(b) Hysteresis energy



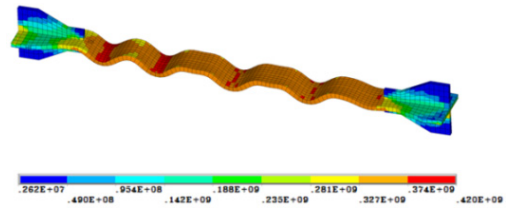
(c) Equivalent damping ratio

Fig. 12 Comparison between simulation and experimental results of mechanical properties of BRB1 with 0.5 mm gap

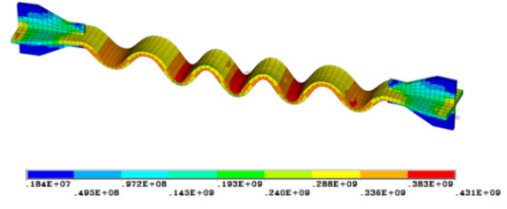


(a) Core element with 0.1 mm gap

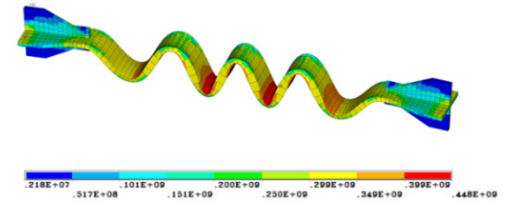
Fig. 13 Deformations of core element and restrained element with different reserved gaps



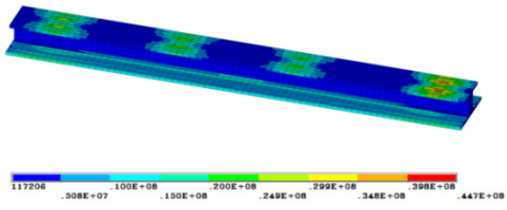
(b) Core element with 0.5 mm gap



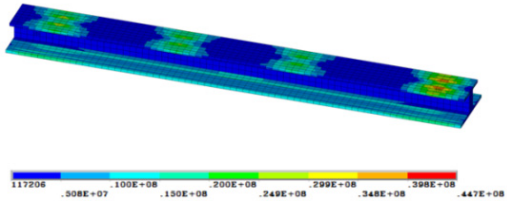
(c) Core element with 1 mm gap



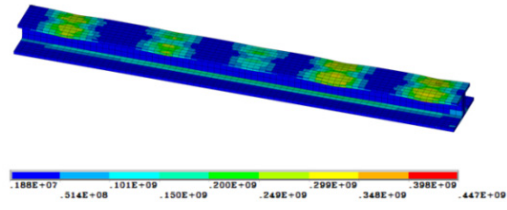
(d) Core element with 2 mm gap



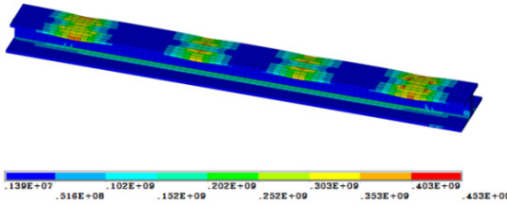
(e) Restrained element with 0.1 mm gap



(f) Restrained element with 0.5 mm gap



(g) Restrained element with 1 mm gap



(h) Restrained element with 2 mm gap

Fig. 13 Continued

5.2 Effect of the reserved gap

In order to study the effect of gap dimension on mechanical properties of BRB1, the reserved gaps between the core element and the restrained element are taken as 0.1 mm, 0.5 mm, 1 mm and 2 mm. Figs. 13(a)-(d) show deformations of the core element with different reserved gaps. It can be seen that the deformation increases rapidly and the stress distribution becomes uneven with the increase of the gap dimension. The energy dissipation section of BRB with the reserved gap of 0.1 mm yields in the total cross section, and the transition section and the connecting section still maintain elastic, which is consistent with the design principle of BRB. Figs. 13(e)-(h) show stresses of the restrained element with different reserved gaps. It can be seen that the contact stress of the restrained element increases with the increase of the gap dimension, which is due to the effect of multi-wave buckling. For the reserved gap of 0.1 mm, the maximum stress of the restrained element reaches 44.7 MPa which is below the yield stress. For the reserved gap of 2 mm, the maximum stress of the restrained element reaches 453 MPa which exceeds the yield stress.

Fig. 14 shows hysteresis curves of BRB1 with different reserved gaps. The hysteresis curve is full and behaves symmetrically in tension and compression states when the gap is only 0.1 mm. But the energy dissipation capacity and stability gradually decrease with the increase of the gap dimension. The curve appears pinching phenomenon when the gap reaches 2 mm, which indicates that BRB1 with large gap has an obvious decline in the energy dissipation

capacity. Fig. 15 shows energy dissipation capacities with different reserved gaps. It can be seen that hysteretic energy and the equivalent damping ratio both decrease with the increase of the reserved gap. Compared to the case of the 2 mm gap, the hysteretic energy values with 0.1 mm gap improve by 36.0%, 33.1%, 39.4% and 37.4% at the four load amplitudes, respectively, and the equivalent damping ratios increase by 19.9%, 25.6%, 27.1% and 20.7%, respectively. The above analysis shows the gap dimension has a significant influence on the energy dissipation performance of BRBs, and the smaller gap can weaken the multi-wave buckling of the core element and then results in the better energy dissipation capacity and stability.

5.3 Effect of the viscoelastic filler

The comparison between BRBs with 2 mm gap and with 2 mm viscoelastic filler can reflect the effect of viscoelastic filler. Fig. 16(a) shows hysteresis curves of BRBs with 2 mm gap and with 2 mm viscoelastic filler. It can be seen that two types of hysteresis curves are basically consistent, but the compression capacity of BRB1 appears a continuous jumping phenomenon with the maximum reduction of 31.3% in compression, but the hysteresis curve of BRB2 is more symmetrical and stable. This is because the restriction and extrusion provided by viscoelastic filler can well weaken the multi-wave buckling deformation of the core element. Figs. 16(b) and (c) show energy dissipation capacities of BRBs with 2 mm gap and with 2 mm viscoelastic filler. It can be seen that, the hysteretic energy and equivalent damping ratio of BRB1 with 2 mm gap are

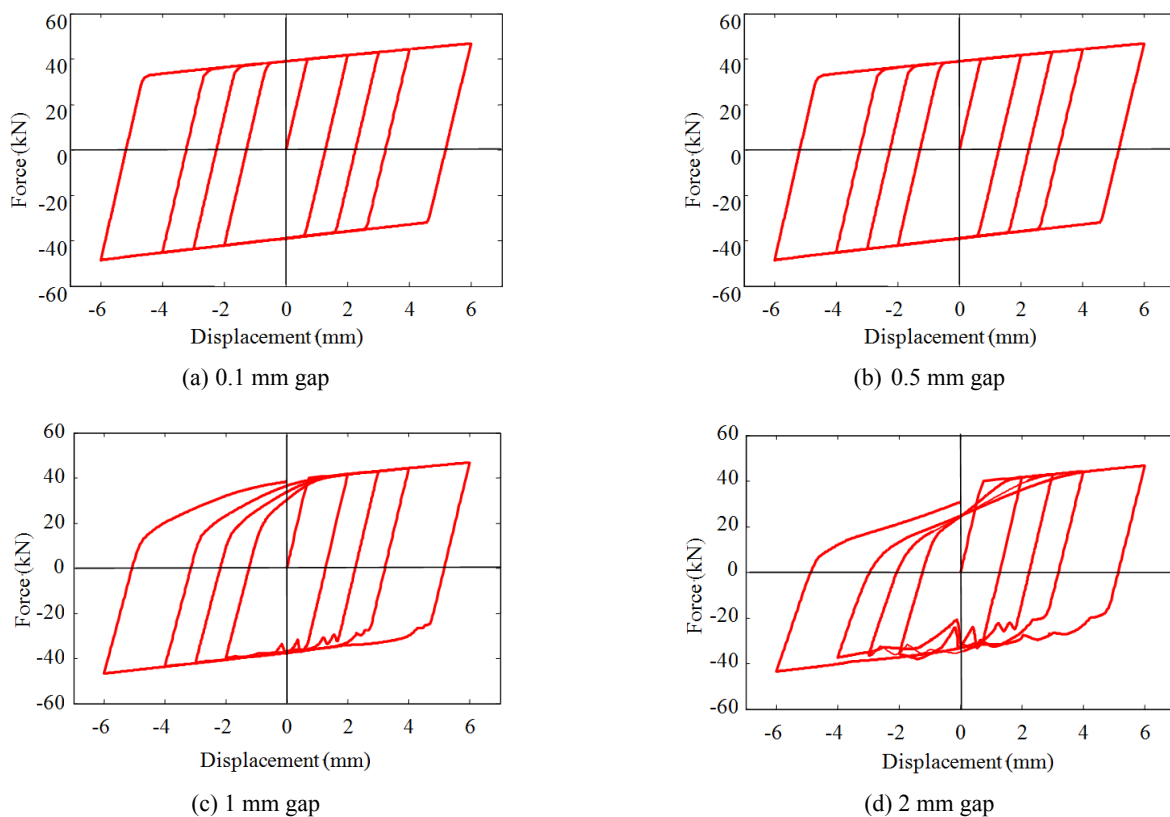


Fig. 14 Hysteresis curves of BRB1 with different reserved gaps

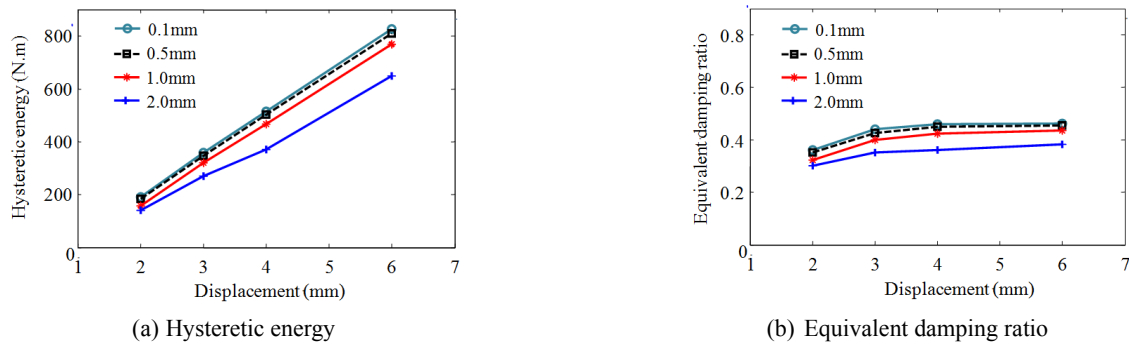


Fig. 15 Mechanical Properties of BRB1 with different reserved gaps

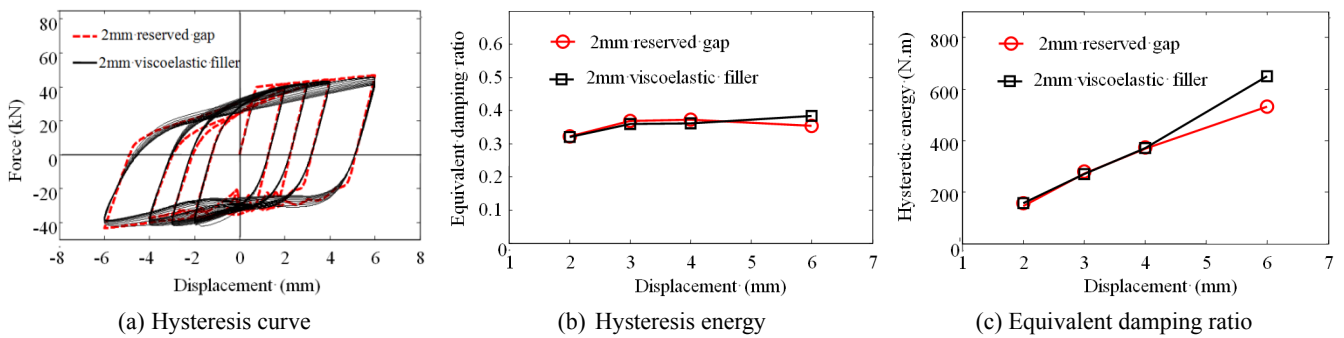


Fig. 16 Comparison between BRB1 with 2 mm gap and BRB2 with 2 mm viscoelastic filler

close to those of BRB2 at the load amplitudes of 2 mm, 3 mm and 4 mm. But at the load amplitude of 6 mm, the hysteretic energy and equivalent damping ratio of BRB2 improve by 22.4% and 8.2% compared to BRB1 with 2 mm gap. Considering that the simulation results slightly enlarges the energy dissipation capacity of BRB1, it can be concluded that the BRB2 with 2 mm viscoelastic filler has the better energy dissipation capacity, especially at the large load amplitude. The main reason is that the severe multi-wave buckling at the large load amplitude will extrude the viscoelastic filler, and the filler reactively restricts the development of the multi-wave buckling. In addition, the friction between the core element and viscoelastic filler generates the energy consumption in repeated tension and compression, which also improves the energy dissipation capacity of BRB2.

6. Conclusions

BRBs with 0.5 mm gap and with 2 mm viscoelastic filler are designed and manufactured, and then the fatigue life prediction model of the two BRBs is proposed. The property tests under different load amplitudes have been carried out, and then the finite element analysis of BRB has also been performed. Based on this study, some conclusions can be drawn as follows:

- The proposed prediction model of fatigue life based on Manson-Coffin model can effectively predict the fatigue life of BRBs with gap or viscoelastic filler,

and the maximum error of 20% can be acceptable. The multi-wave buckling deformation significantly affects the fatigue life of BRBs and cannot be ignored.

- Experimental results show that BRB with 2 mm viscoelastic filler has the better mechanical stability and fatigue properties compared to BRB with 0.5 mm gap. The viscoelastic filler employed in BRB can provide the expansion space for inner core element, reduce the friction between inner core element and outer restrained element, and generate energy consumption in repeated tension and compression, especially at the large load amplitude.
- Finite element analysis indicates the smaller reserved gap can effectively improve the energy dissipation performance of BRBs, and BRB with 2 mm viscoelastic filler has the better energy dissipation capacity and stability than BRB with 2 mm gap.

Acknowledgments

Financial supports for this research are provided by National Science Fund for Distinguished Young Scholars (51625803), China and Korea international cooperation project of the national key research and development program (2016YFE0119700), National Natural Science Fund of China (11572088), Key Research and Development Plan of Jiangsu Province (BE2015158), Talent Training Foundation of Southeast University (CE02-1-49). These supports are gratefully acknowledged.

References

- Abdollahzadeh, G. and Banihashemi, M. (2013), "Response modification factor of dual moment-resistant frame with buckling restrained brace (BRB)", *Steel Compos. Struct., Int. J.*, **14**(6), 621-636.
- AISC (American Institute of Steel Construction) (2010), "Seismic provisions for structural steel building", *ANSI/AISC 341-10*, Chicago, IL, USA.
- Bregoli, G., Genna, F. and Metelli, G. (2016), "Analytical estimates for the lateral thrust in bolted steel buckling-restrained braces", *J. Mech. Mater. Struct.*, **11**(2), 173-196.
- Chen, Q., Wang, C.L., Meng, S. and Zeng, B. (2016), "Effect of the unbonding materials on the mechanic behavior of all-steel buckling-restrained braces", *Eng. Struct.*, **111**, 478-493.
- Chou, C.C. and Chen, S.Y. (2010), "Subassembly tests and finite element analyses of sandwiched buckling-restrained braces", *Eng. Struct.*, **32**(8), 2108-2121.
- Coffin, L.F.Jr. (1954), "A study of the effects of cyclic thermal stresses on a ductile metal", *Trans. ASTM*, **76**, 931-950.
- Ding, Y.K., Zhang, Y.C. and Zhao, J.X. (2009), "Tests of hysteretic behavior for unbonded steel plate brace encased in reinforced concrete panel", *J. Constr. Steel Res.*, **65**(5), 1160-1170.
- Ghowsi, A.F. and Sahoo, D.R. (2015), "Fragility assessment of buckling-restrained braced frames under near-field earthquakes", *Steel Compos. Struct., Int. J.*, **19**(1), 173-190.
- Gong, S. and Zhou, Y. (2016), "Experimental study and numerical simulation on a new type of viscoelastic damper with strong nonlinear characteristics", *Struct. Control Health Monit.*
DOI: 10.1002/stc.1897
- Kim, D.H., Ju, Y.K., Kim, M.H. and Kim, S.D. (2014), "Wind-induced vibration control of tall buildings using hybrid buckling-restrained braces", *Struct. Des. Tall Spec. Build.*, **23**(7), 549-562.
- Manson, S.S. (1965), "Fatigue: A complex subject—some simple approximations", *Exp. Mech.*, **5**(7), 193-226.
- Metelli, G., Bregoli, G. and Genna, F. (2016), "Experimental study on the lateral thrust generated by core buckling in bolted-BRBs", *J. Constr. Steel Res.*, **122**, 409-420.
- Miner, M.A. (1945), "Cumulative damage in fatigue", *J. Appl. Mech. ASME*, **12**(3), 159-164.
- Park, J., Lee, J. and Kim, J. (2012), "Cyclic test of buckling restrained braces composed of square steel rods and steel tube", *Steel Compos. Struct., Int. J.*, **13**(5), 423-436.
- Soong, T.T. and Dargush, G.F. (1997), *Passive energy dissipation systems in structural engineering*. John Wiley and Sons Ltd., UK.
- Soong, T.T. and Spencer, B.F. (2002), "Supplemental Energy Dissipation: state-of-the-art and state-of-the-practice", *Eng. Struct.*, **24**(3), 243-259.
- Takeuchi, T., Hajar, J.F., Matsui, R., Nishimoto, K. and Aiken, I.D. (2012), "Effect of local buckling core plate restraint in buckling restrained braces", *Eng. Struct.*, **44**, 304-311.
- Talebi, E., Tahir, M.M., Zahmatkesh, F. and Kueh, A.B. (2015), "A Numerical analysis on the performance of buckling restrained braces at fire-Study of the gap filler effect", *Steel Compos. Struct., Int. J.*, **19**(3), 661-678.
- Tsai, K.C., Wu, A.C., Wei, C.Y., Lin, P.C., Chuang, M.C. and Yu, Y.J. (2014), "Welded end-slot connection and debonding layers for buckling-restrained braces", *Earthq. Eng. Struct. Dyn.*, **43**(12), 1785-1807.
- Wang, C.L., Usami, T. and Funayama, J. (2012), "Improving low-cycle fatigue performance of high-performance buckling-restrained braces by toe-finished method", *J. Earthq. Eng.*, **16**(8), 1248-1268.
- Watanabe, A., Hitomi, Y., Saeki, E., Wada, A. and Fujimoto, M. (1988), "Properties of brace encased in buckling-restraining concrete and steel tube", *Proceedings of Ninth World Conference on Earthquake Engineering*, International Association for Earthquake Engineering, Vol. 4, Tokyo-Kyoto, Japan, pp. 719-724.
- Xie, Q. (2005), "State of the Art of Buckling-restrained Braces in Asia", *J. Constr. Steel Res.*, **61**(6), 727-748.
- Xu, Z.D., Wang, D.X. and Shi, C.F. (2011), "Model, Tests and application design for viscoelastic dampers", *J. Vib. Control*, **17**(9), 1359-1370.
- Xu, Z.D., Liao, Y.X., Ge, T. and Xu, C. (2016), "Experimental and theoretical study on viscoelastic dampers with different matrix rubbers", *J. Eng. Mech.*
DOI: 10.1061/(ASCE)EM.1943-7889.0001101, 04016051
- Zhao, J., Wu, B. and Ou, J. (2011), "A novel type of angle steel buckling-restrained brace: Cyclic behavior and failure mechanism", *Earthq. Eng. Struct. Dyn.*, **40**(10), 1083-1102.

CC